Effect of Particulate Size on the Microstructural Evolution, Aging Behavior and Mechanical Properties of Al-4.5Cu/SiC Composites

M. Gupta, M.O. Lai and N.S. Herng

Department of Mechanical and Production Engineering
National University of Singapore, 10 Kent Ridge Crescent, Singapore 119260

ABSTRACT

In the present study, an aluminum based metallic matrix (Al-4.5wt.% Cu) was successfully reinforced with SiC particulates of two different sizes using an innovative disintegrated melt deposition technique. The results of microstructural characterization studies revealed that smaller SiC particulates (8 μm) lead to a more equiaxed matrix grain morphology when compared to the larger SiC particulates (34.4 μm). The matrix grain morphology results were rationalized in terms of particulate-size influenced movement and destabilization of the solid-liquid interface. The results of the aging studies revealed an accelerated aging kinetics in the case of composite samples containing 8 μm SiC particulates when compared to the composite samples with 34.4 μm SiC particulates and unreinforced samples. The accelerated aging kinetics which is unusual in case of aluminum matrices containing copper in excess of 4 weight percent was rationalized in terms of particulate size associated variation in microstructural features. Results of ambient temperature mechanical tests revealed an increase in 0.2% yield strength and decrease in ultimate tensile strength and ductility in the case of composite samples when compared to the unreinforced samples in the as-processed condition. The mechanical properties characterization results were found to reveal direct correlation with the variation in microstructural features of the metallic matrix such as grain size and dislocation density originating due to the presence and different sizes of SiC particulates.

Keywords: Disintegrated melt deposition; grain morphology; aging kinetics; mechanical behavior

INTRODUCTION

The potential of metal matrix composites (MMCs) as promising candidate for critical and non-critical engineering applications has primarily been attributed to their ability to unify the useful properties of metallic and ceramic materials /1/. In order to fully harness the potential of MMCs it is important to select judiciously the processing technique, metallic matrix, reinforcement and the heat treatment procedure /2-4/ placing special emphasis on the nature of end application. Among these variables, the selection of reinforcing phase is of paramount importance and may embody additional efforts since the same type of reinforcement with either different morphology or size can significantly affect the microstructure and hence the properties of the resultant composite material. In related studies, for example, investigators have extensively reported the effect of type /3-5/ and morphological aspects of reinforcement /6/ on the mechanical properties of MMCs. In addition, studies /2, 7-9/ were also carried out to correlate the effect of size of reinforcement with the compressive and tensile properties of the MMCs. Despite these correlative studies, no systematic studies were carried out in order to correlate the effect of particulate size on the microstructural evolution and the microstructurally influenced aging response and mechanical properties of composites.

Accordingly, in the present study an attempt was made to synthesize Al-4.5 Cu based MMCs reinforced with two different sizes of SiC particulates using an innovative disintegrated melt deposition (DMD) technique. Microstructural characterization studies were conducted using optical and scanning electron microscopes while tensile testing was carried out using an automated servohydraulic Instron testing machine. Particular emphasis was placed to correlate the microstructural evolution, aging response and the mechanical properties of the MMCs with the size of SiC particulates.

EXPERIMENTAL PROCEDURE

Materials

The nominal composition of the matrix alloy used in the present study was (in wt. %): 4.5Cu - Al (bal.). Silicon carbide (α-SiC) particulates with an average sizes of 34.4 μm and 8 μm were selected as the reinforcement phase.

Processing

The first step in the synthesis of the metal matrix composites using the DMD technique involved cleaning of the starting elemental materials prior to melting in order to eliminate surface impurities. The cleaned elemental materials were taken in graphite crucible and superheated to 950°C. SiC particulates (equivalent to 10 wt. %) preheated to 900°C were then added into the molten metal stirred using an impeller. The stirring time of SiC particulates in the melt was maintained between 10 and 15 minutes. The composite melt was then disintegrated using argon gas at 0.18 m from the melt pouring point under inert atmospheric conditions. The gas flow rate was maintained at 4.17 x 10^{-4} m^3/s. The disintegrated composite melt slurry was subsequently deposited on a circular shaped metallic substrate located at 0.25 m from the gas disintegration point. For the purpose of comparison, the base alloy superheated to 950°C was also synthesized using similar processing conditions.

It may be noted that the fundamental scientific principles behind the disintegrated melt deposition technique are similar to those of spray atomization and deposition and Osprey forming techniques /3,5/; however, it differs completely with respect to particulate injection in metallic melt, melt disintegration point, melt deposition mode and that the end product is only bulk composite material /10/. A process yield (in terms of the bulk composite material) up to 80% has been obtained using the present methodology owing to the complete absence of overspray powders.

Quantitative Assessment of SiC Particulates

Quantitative assessment of SiC particulates in the DMD processed samples was carried out using a chemical dissolution method. This method involved: i) measuring the mass of composite samples, ii) dissolving the samples in hydrochloric acid, followed by iii) filtering to separate the ceramic particulates. The particulates were then dried and the weight fraction determined /5, 10, 11/.

Density measurement

Density measurements were carried out in order to ascertain the volume fraction of porosity in the unreinforced and reinforced samples. Density measurements were carried out using Archimedes' principle following the procedure as discussed in References /5,10,11/.

Aging Studies

Aging studies were carried out in order to obtain the peak hardness time for the unreinforced and metal matrix composite samples. The DMD processed specimens (25 mm diameter x 7 mm height) were solutionized for one hour at 540°C, quenched in cold water and aged at 160°C for various intervals of time. Rockwell superficial hardness measurements were made using a 1.58 mm diameter steel ball indenter with a 15 kg load using a GNEHM HORGEN digital hardness tester following ASTM standard E18-92. A minimum of three hardness readings were taken for each specimen.

Microstructural Characterization

Microstructural characterization studies were conducted on the peak aged unreinforced and

reinforced samples in order to investigate the grain size, grain morphology, presence of porosity and the distribution of SiC particulates.

Microstructural characterization studies were primarily accomplished using an optical and a JEOL scanning electron microscope equipped with EDS [Energy Dispersive Spectroscopy]. The unreinforced and composite samples were metallographically polished prior to examination. Microstructural characterization of the samples was conducted in both etched and unetched conditions. Etching was accomplished using Keller's reagent [0.5 HF - 1.5 HCl - 2.5 HNO_3 - 95.5 H_2O]. The grain size measurements were carried out using the linear intercept method, as described in ASTM E 112-84.

Mechanical Behavior

The smooth bar tensile properties were determined on the peak aged monolithic and composite specimens following ASTM standard E8M-91. Tensile tests were conducted using an automated servohydraulic Instron testing machine on round tension test specimens of 4 mm diameter and 20 mm gage length using an initial strain rate of 2.1×10^{-4} s^{-1}.

Fracture Behavior

Fracture surface characterization studies were carried out on the tensile fractured unreinforced and reinforced samples in order to provide insight into the various fracture mechanisms operative during tensile loading of the peak aged samples. Fracture surface characterization studies were primarily accomplished using a JEOL scanning electron microscope equipped with EDS.

RESULTS

Macrostructure

The overall dimensions of the disintegrated melt deposited composite preforms were approximately 0.035 m in height and 0.055 m in diameter. The specimens for microstructural and mechanical properties characterization were removed randomly across the DMD processed preforms after ensuring the microstructural homogeneity.

Quantitative Assessment of SiC Particulates

The results of acid dissolution experiments are summarized in Table 1. The weight percentages of SiC particulates was estimated to be approximately 8.8 % for Al-4.5Cu/8μm SiC specimens and 9.6 % for the Al-4.5Cu/34.4μm SiC specimens.

Density measurement

The results of density measurements conducted on the as-processed unreinforced and composite specimens reinforced with 8 μm and 34.4 μm SiC particulates revealed density values of 2.77, 2.70 and 2.67 g cm^{-3} respectively. The volume percent of the porosity computed using the experimentally determined density values and the results of acid dissolution tests are shown in Table 1.

Table 1
Results of the Quantitative Microstructural Characterization

Matrix	SiC Size (μm)	Wt.% SiC	Porosity (vol. %)	Grain Size (μm)	Roundness of Grains*	Cluster Size (μm)
Al-4.5Cu	--	--	0.75	236 ± 34.0	2.02 ± 0.46	--
Al-4.5Cu	8	8.8	4.60	53 ± 3.4	1.70 ± 0.42	31.8 ± 9.6
Al-4.5Cu	34.4	9.6	5.78	86 ± 10.2	1.71 ± 0.56	148.7 ± 42.5

*Roundness = $(\text{perimeter})^2/4\pi$ Area. Determined using image analysis.

Aging Studies

The results of aging studies conducted on the unreinforced and composite samples are shown in Fig. 1. The results exhibit the presence of a well-defined hardness peak at 12 hrs for the unreinforced samples and Al-4.5Cu/34.4μm SiC samples and at 9 hrs for the Al-4.5Cu/8μm SiC samples. The results also reveal that the maximum as-quenched and peak hardness is achieved in the composite samples containing 8 μm SiC particulates followed by the composite samples containing 34.4 μm SiC particulates and lastly the unreinforced samples.

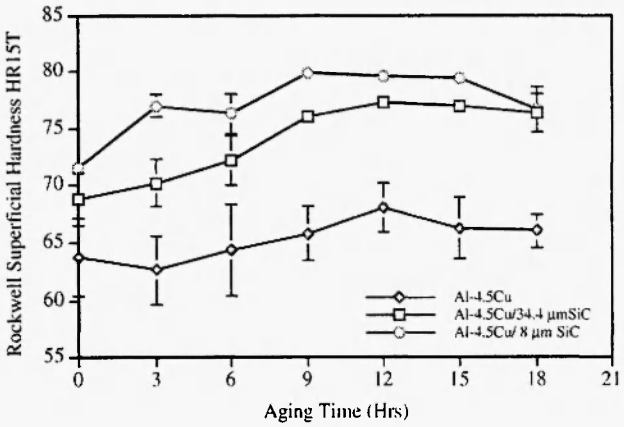

Fig. 1: Graphical representation of aging studies conducted on unreinforced and reinforced samples.

Microstructural Characterization

Scanning electron microscopy conducted on unetched and etched unreinforced Al-4.5Cu samples revealed the presence of: predominantly columnar and partly equiaxed matrix microstructure, minimal amount of micrometer sized porosity and interdendritically located Cu rich intermetallic phase. A representative micrograph taken from the unreinforced sample is shown in Fig. 2.

The microstructural characterization studies conducted on the Al-4.5Cu/34.4μm SiC samples revealed dendritic/equiaxed matrix microstructure (see Fig. 3a). The roundness [(perimeter)^2/4π area] which determines the columnar extent of grains was however

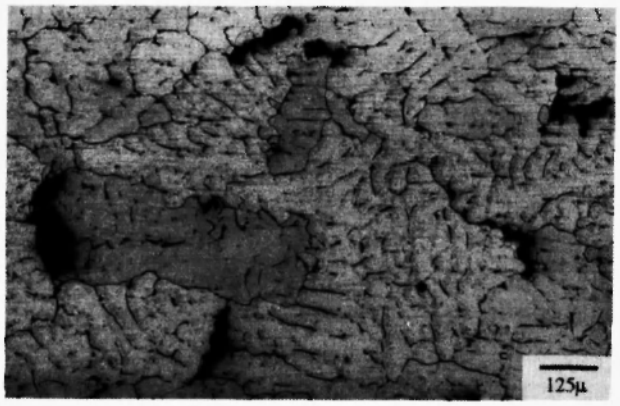

Fig. 2: Representative SEM micrograph showing the microstructural features observed in the DMD processed Al-4.5Cu samples.

less when compared to the unreinforced samples (see Table 1). The interdendritic/intercellular regions were found to be frequently associated with the presence of Cu rich phases. The metallic matrix also revealed the presence of porosity predominantly associated with short edges and angular locations of SiC particulates and with SiC clusters. The distribution of SiC particulates in the matrix can be assessed from Fig. 3b. The interfacial integrity between SiC particulates and Al-Cu matrix was found to be good (see Fig. 3c) and in some cases metal free zones (pores) as mentioned above were also observed at angular locations. In addition, the interface formed between the SiC particulates and Al-Cu matrix also revealed the presence of Cu-rich secondary phases.

Finally, the results of microstructural characterization studies conducted on the composite samples containing 8 μm SiC particulates revealed an increasingly equiaxed (reduced average roundness of the grains) (see Table 1) matrix microstructure; grain boundary segregated distribution of SiC particulates; lower cluster size to particulate ratio; superior interfacial integrity and presence of Cu rich phases in the near vicinity of SiC particulates (see Fig. 4).

Mechanical Behavior

The results of ambient temperature testing on the unreinforced and DMD processed composite samples,

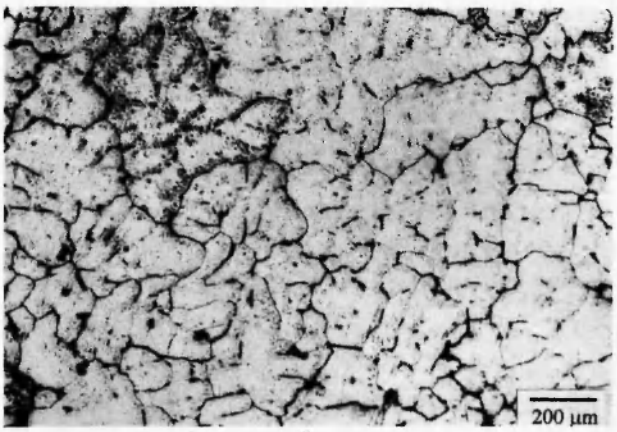

a

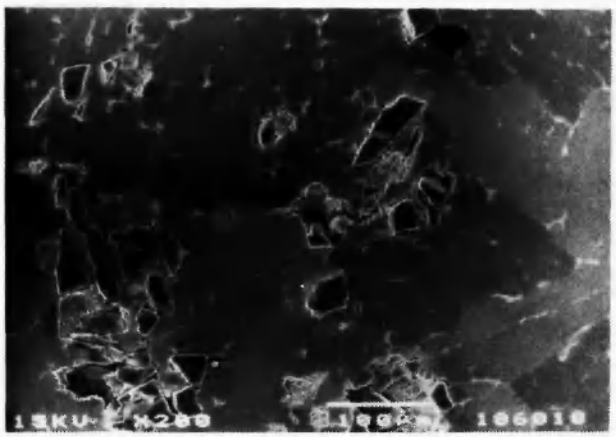

b

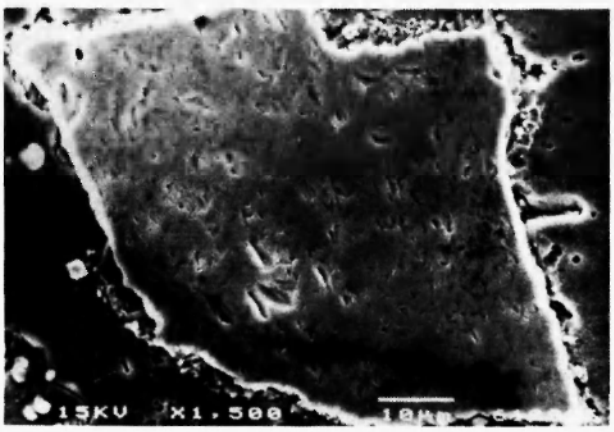

c

Fig. 3: Representative micrographs showing: a) grain morphology, b) matrix microstructure, and c) interfacial integrity between SiC particulate and metallic matrix in the case of Al-4.5Cu/34.4µm SiC samples.

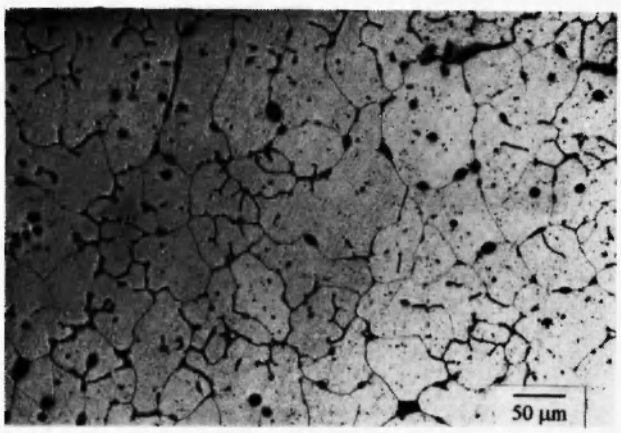

a

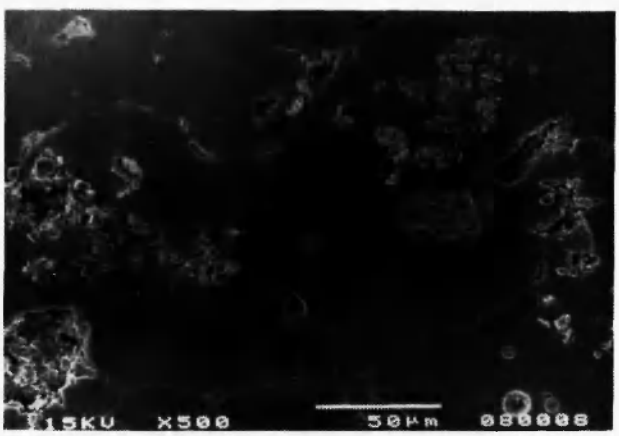

b

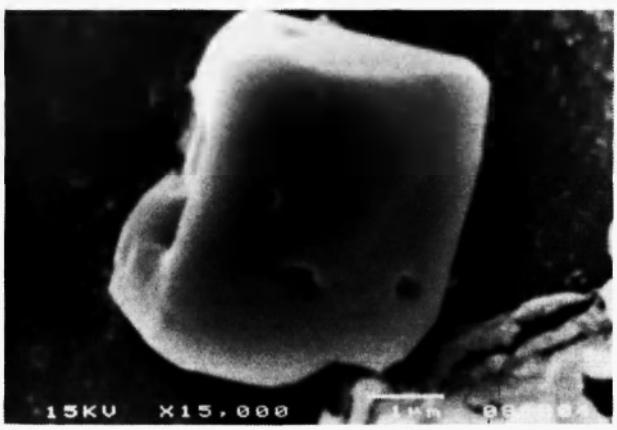

c

Fig. 4: Representative micrographs showing: a) grain morphology, b) matrix microstructure, and c) interfacial integrity between SiC particulate and metallic matrix in the case of Al-4.5Cu/8µm SiC samples.

Table 2
Results of Room Temperature Mechanical Properties

Material	SiC. Size (μm)	Condition	0.2 % YS (MPa)	UTS (MPa)	Ductility (%)
Al-4.5Cu	--	Peak aged	104.2 ± 2.0	232.0 ± 12.0	10.7 ± 1.5
Al-4.5Cu	8	Peak aged	167.2 ± 2.9	200.4 ± 7.8	2.2 ± 0.5
Al-4.5Cu	34.4	Peak aged	118.7 ± 51.3	181.4 ± 50.4	2.5 ± 0.4

aged to peak hardness, are summarized in Table 2. The results in Table 2 show that composite samples exhibited higher 0.2% yield stress (0.2% YS) and reduced ultimate tensile strength (UTS) and ductility when compared to the unreinforced samples. Regarding the effect of particulate size, the composite samples with 8 μm particulate size exhibited higher 0.2% YS, UTS and slightly lower ductility when compared to composite samples containing 34.4 μm size SiC particulates.

Fracture Behavior

The tensile fracture surfaces of unreinforced and reinforced samples are shown in Fig. 5. The fractographs taken from the unreinforced samples revealed the presence of dimples indicative of a predominantly ductile failure (see Fig. 5a). Fracture studies conducted on the tensile fracture surface of the Al-4.5Cu/34.4μm SiC samples revealed the presence of dimples indicative of the ductile nature of matrix deformation, frequently observed cracked SiC particulates (see Fig. 5b), evidence of SiC interfacial debonding and presence of SiC clusters. Finally, fractographic analysis conducted on Al-4.5Cu/8μm SiC samples revealed the presence of dimples, minimal evidence of SiC particulate cracking, frequently observed debonded SiC particulates (see Fig. 5c) and presence of SiC clusters on the fractured surface.

DISCUSSION

Microstructure

The microstructure of the unreinforced samples and DMD processed composite samples revealed three common salient features:

a) the presence of columnar / equiaxed matrix microstructure,

b) the presence of porosity, and

c) the presence of interdendritic Cu-rich phase.

The presence of columnar-equiaxed matrix microstructure (also known as "ingot" type structure) in case of unreinforced and reinforced samples indicates that the remaining liquid temperature after the onset of solidification from the nucleation sites remained above the nucleation temperature. The underlying principles behind the development of "ingot" type of structure are well established and can be found elsewhere /12/. Beside exhibiting columnar/equiaxed grain structure in common, the results of the present study also indicated that the extent of columnar grain formation was maximum in case of unreinforced samples, relatively less in case of Al-4.5Cu/34.4μm SiC samples and minimum in case of Al-4.5Cu/8μm SiC samples. The tendency for the columnar to equiaxed grain formation may vary depending on the characteristics of the processing methodology /13-16/. For example, the columnar to equiaxed transition in the case of unreinforced alloys solidifying under equilibrium or near equilibrium conditions may be attributed to /13/: a) decrease in the pouring temperature, b) increase in the alloying content, and c) increase in the rate of cooling. Various theories were proposed to provide insight into the formation of equiaxed grains and can be found elsewhere /13,14/. For non equilibrium

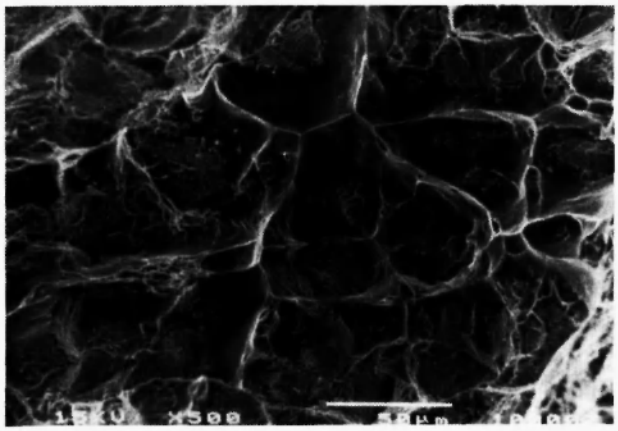

a

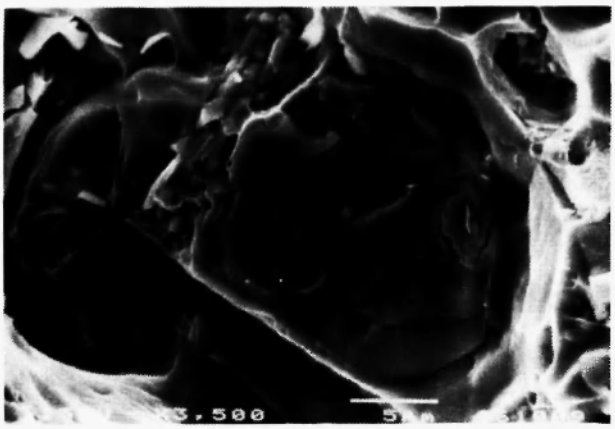

b

c

Fig. 5: Typical SEM micrographs showing fracture surface characteristics of: a) unreinforced samples showing the presence of dimples, b) Al-4.5Cu/34.4μm SiC samples showing particulate breakage and c) Al-4.5Cu/8μm SiC samples showing partially debonded SiC particulate.

processing methods such as spray atomization and deposition, the formation of equiaxed grains in both the unreinforced and reinforced materials was attributed to: a) dendrite arm fragmentation, b) nucleation/grain multiplication, and c) constrained growth /15,16/. The relatively smaller grain size exhibited by reinforced samples when compared to the unreinforced samples was attributed to the presence of ceramic reinforcement and its ability to increase the heat transfer prior to and during solidification and to pin the grain boundaries during solid state cooling /5,17/. Disintegrated melt deposition processing besides being based on similar processing fundamentals as that of spray processes used by investigators elsewhere /18-23/ is a near equilibrium process as evidenced by its columnar-equiaxed matrix microstructure /10/. During disintegrated melt deposition processing, since the processing variables such as pouring temperature, alloying content and deposition conditions were similar for all the unreinforced and reinforced samples, the most likely cause of the decreased tendency of the columnar nature of grains from unreinforced to Al-4.5Cu/34.4μm SiC to Al-4.5Cu/8μm SiC samples can be attributed to the presence and size of SiC particulates. Based on the microstructural characterization results obtained in the present study, the reduced tendency of the columnar grain formation can be attributed to the increase in constraint towards the growth of the primary metallic phase (α-Al) by the presence of SiC particulates as in the case of composite samples when compared to the unreinforced samples /24/. Among the composite samples, the comparatively lesser tendency of columnar grain formation exhibited by Al-4.5Cu/8μm SiC samples can be attributed to the relatively higher constraint offered by 73 times the number of SiC particulates in front of solid-liquid interface when compared to the Al-4.5Cu/34.4μm SiC samples. It may be noted that the number of particulates in each case was computed by taking the ratio of total weight of SiC particulates in the sample to the weight of an individual SiC particulate (see also Table 1). Moreover, the reduced tendency of columnar grain formation exhibited by composite samples and particularly the Al-4.5Cu/8μm SiC samples can also be attributed to the ability of SiC particulates to destabilize the solid-liquid interface and the superior ability of finer SiC par-

ticulates (<10 μm) to influence the thermal field as a result of added effect of microconvection to the mostly buoyancy driven convection applicable to large particulates /25,26/. In addition to the variation in the morphological aspects of the grains, the results of the present study also indicated that the unreinforced samples revealed maximum grain size followed by Al-4.5Cu/34.4μm SiC samples and lastly the Al-4.5Cu/8μm SiC samples. The smaller grain size exhibited by composite samples when compared to the unreinforced samples may primarily be attributed to the grain boundary pinning effect of SiC particulates during solid state cooling. These results are consistent with the similar findings of other investigators obtained on spray deposited unreinforced and reinforced 2519 Al alloys /5/. Finally, the superior ability of 8 μm SiC particulates to refine the grain size may be attributed to their large number (approximately 73 times the number of 34.4 μm SiC particulates) resulting in an increase in grain boundary pinning sites.

Another important microstructural feature observed in case of unreinforced and reinforced samples investigated in the present study was the presence of porosity. Both unreinforced and reinforced samples exhibited, in common, the presence of microporosity in the metallic matrix and the reinforced samples, in addition, also exhibited the presence of metal free zones at sharp corners of SiC particulates and within SiC clusters. The formation of microporosity under the experimental conditions used in the present study was inevitable primarily as a result of columnar-equiaxed type of solidification structure exhibited by unreinforced and reinforced samples. The mechanisms associated with the formation of porosity during solidification of materials exhibiting columnar-equiaxed type of structure have been previously established and can be found elsewhere /12/. Regarding the amount of porosity, the higher volume percent of porosity observed in composite samples can primarily be attributed to higher viscosity of the composite slurry when compared to the metallic melt /25/ and its subsequent effect on the formation of metal free zones at the sharp corners of the SiC particulates and within the SiC clusters /10, 27/. The higher volume percent of porosity exhibited by Al-4.5Cu/34.4μm SiC samples when compared to Al-4.5Cu/8μm SiC samples can be attributed to the higher cluster forming tendency exhibited by 34.4 μm SiC particulates (see Table 1). The origin of metal free zones within SiC clusters has previously been established in the analogous studies /10, 27/.

The presence of the interdendritic/intercellular Cu-rich phase observed in case of unreinforced and composite samples can be attributed to the sluggish solidification front velocity achieved during primary processing of materials, rejection of Cu ahead of the moving liquid-solid interface and subsequent solidification when the temperature of the remaining liquid reached the eutectic temperature /10-12, 27,28/.

Distribution of SiC particulates

The results of the distribution studies revealed that the SiC particulates in both types of composites samples were predominantly located at the grain boundaries. The grain boundary segregation of SiC particulates can primarily be attributed to:

i) the inability of SiC particulates to serve as nucleation site for the primary α-Al phase solidification /29, 30/ and
ii) the inability of the solidification front to achieve velocity higher than the critical velocity required for the engulfinent of SiC particulate /17,31/.

Further work is continuing to delineate the factors responsible for higher cluster forming tendency exhibited by composite samples containing 34.4 μm size SiC particulates when compared to the composite samples containing 8 μm size SiC particulates.

Interfacial Characteristics

The results of the present study indicated that SiC-Al matrix interfacial integrity (assessed in terms of interfacial debonding and presence of voids), under similar processing conditions, was comparatively poor in the case of Al-4.5Cu/34.4μm SiC samples when compared to that in Al-4.5Cu/8μm SiC samples. The inferior SiC-Al matrix interfacial integrity observed in Al-4.5Cu/34.4μm SiC samples can primarily be attributed to the higher viscosity of the composite slurry

and its inability to negotiate sharp corners associated with SiC particulates. It may be noted that higher viscosity of the composite slurry in case of Al-4.5Cu/34.4μm SiC samples can be attributed to the higher weight percent of SiC particulates when compared to Al-4.5Cu/8μm SiC samples (see Table 1). The increase in viscosity of the metallic melt with an increase in volume fraction of particulates has previously been established by other investigators /25/.

Another important microstructural characteristic associated with the Al-Cu/SiC interfacial region in composite samples was the presence of Cu-rich secondary phases (see Figs 3c and 4c). The presence of secondary phases in the interfacial region demonstrate the capability of the dislocation defect structure in the interfacial region in providing preferential sites for heterogeneous nucleation when compared to the bulk matrix /5/. The results are consistent with the experimental findings of other investigators obtained on Al-Cu based metal matrix composites using scanning and transmission electron microscopy techniques /5,10,27/. Further work is continuing in order to identify the composition and structural aspects of these secondary phases.

Aging Studies

Aluminum-copper based alloys are amongst the most commonly used alloys in their unreinforced form and more recently as metallic matrices in composite materials /3-6,10/. An understanding of the aging behavior of these alloys is of paramount importance since it provides valuable information regarding the temperature and time combination that is required in order to achieve either underaged, peak aged or overaged conditions. In the past, Al-Cu based alloys were extensively studied to establish mechanisms of hardening /32-34/ and more recently to study the influence of presence of ceramic reinforcement on the precipitation sequence and kinetics /35-37/. For binary Al-Cu alloys the precipitation sequence can be represented as /32,33/:

supersaturated solid solution → coherent G.P. zones → metastable θ" coherent phase → metastable θ' semi-coherent phase → equilibrium θ ($CuAl_2$) incoherent phase.

This precipitation sequence, however, can be realized under equilibrium aging conditions and may vary with a number of factors. One of the common factors that influences the aging kinetics of both the unreinforced and reinforced Al-Cu based alloys is the temperature of aging /33,36/. An increase in aging temperature, for example, leads to a decrease in the time required for achieving peak hardness and suppresses the formation of G.P. zones /33,36/ in both the unreinforced and reinforced Al-Cu based alloys. Amongst other factors that influence aging kinetics of the Al-Cu based alloys include the type of processing, type of reinforcement, and the volume fraction of the reinforcement /35-37/.

In this work, the results of the aging studies reveal that the as-quenched and peak hardness of the metal matrix composite samples is higher than that of their monolithic counterpart. This can be attributed to:

a) higher dislocation density present in the composite matrix as a result of the mismatch between the coefficient of thermal expansion of the metallic matrix and the ceramic reinforcement /5,38/, and
b) pronounced matrix microstructural refinement in the composite samples as evidenced from the reduction in grain size (see Table 1)

The relatively higher hardness exhibited by Al-4.5Cu/8μm SiC samples when compared to the Al-4.5Cu/34.4μm SiC samples besides having lesser weight percentage can be attributed to the coupled influence of:

a) superior ability of 8 μm SiC particulates to increase the dislocation density in the metallic matrix when compared to 34.4 μm SiC particulates /2/,
b) superior ability of 8 μm SiC particulates to refine grain size (see Table 1) that can be attributed to their relatively more uniform distribution and lower SiC clusters to particulate size ratio in the metallic matrix, and
c) lower amount of porosity (see Table 1)

The results of the aging studies also revealed that Al-Cu matrix reinforced with 8 μm SiC particulates exhibited accelerated aging kinetics when compared to the unreinforced samples and Al-4.5Cu/34.4μm SiC

samples. In similar studies, investigators reported similar aging kinetics exhibited by AA2519 matrix (Al-5-7 wt.% Cu) even when reinforced with SiC or Al_2O_3 particulates /5/ while Kim *et al.* /37/ reported the suppression in aging kinetics of a Al-4 wt.% Cu matrix reinforced with up to 15 wt. % SiC whiskers. The retardation in aging kinetics was attributed to the suppression in θ" as a result of the presence of SiC whiskers. The accelerated aging kinetics observed in case of composite samples containing 8 μm SiC particulates especially when compared to composite samples containing 34.4 μm SiC particulates can be attributed to the conjunct influence of a number of factors such as:

a) decrease in grain size (See Table 1),
b) reduced particulates' associated porosity,
c) relatively more uniform distribution of SiC particulates as evidenced by lower clusters to particulate size ratio, and
d) large number of SiC particulates and associated increased number of heterogeneous nucleation sites.

The accelerated aging can be explained, in part, by the increase in grain boundary area (as a result of 0.62 times the grain size of Al-4.5Cu matrix containing 8 μm SiC particulates when compared to the grain size of Al-Cu matrix with 34.4 μm SiC particulates) and its ability to promote the nucleation of the strengthening phases as a result of the reduced activation barrier for the heterogeneous nucleation /33/. The experimental confirmation of the heterogeneous nucleation of the precipitates at the grain boundaries in case of Al matrices has been established previously /5,39/.

The minimal presence of porosity at the matrix-SiC interfaces as in the case of composite samples with 8 μm SiC particulates may also encourage accelerated aging kinetics by assisting the sequential events involving: generation of misfit strains due to difference in coefficient of thermal expansion between SiC particulates and matrix /22,40/, punching of dislocations in the matrix /38/, and the subsequent heterogeneous nucleation of the strengthening phases in the matrix. The presence of porosity at the particulates' interface, that was relatively more prominent in the case of composite samples containing 34.4 μm SiC particulates, reduces misfit strains as a result of the ability of SiC particulate to adjust itself in the metal free space (porosity) during quenching, resulting in a lower dislocation density and hence a reduced amount of heterogeneous nucleation volume around the particulates /38,40,41/ thus retarding the rate of precipitation. The results are consistent with the work of other investigators /42/ showing lesser extent of segregation of copper in the near vicinity of porosity-associated SiC particulates.

The accelerated aging kinetics exhibited by Al-4.5Cu/8μm SiC samples can also be attributed to the more uniform distribution of SiC particulates and relatively smaller size of SiC clusters. In analogous studies /42/, for example, investigators showed that the uniform distribution of SiC particulates achieved by using different processing technique assisted in accelerating the aging kinetics. This was essentially rationalized in terms of reduced ability of SiC particulates present in clusters to punch dislocations in the matrix when compared to SiC particulates present individually in the matrix. The diminishing ability of SiC particulates present in clusters to punch dislocations reduces the nucleation tendency of the strengthening phases in the near vicinity of SiC particulates (and thus does not help in accelerating aging kinetics) as a result of: i) reduced segregation of alloying elements in the matrix adjacent to SiC particulates and thus the compositional requirement for formation of precipitates /41/, and ii) reduced heterogeneous nucleation sites in the form of dislocations. It may be noted that SiC clusters are often associated with the presence of porosity /42/ and this enables the individual SiC particulates in the cluster to readjust themselves when acted upon by the compressive forces during quenching from the solutionizing temperatures, thus reducing the extent of misfit strains in the adjacent matrix.

Finally, the accelerated aging kinetics exhibited by Al-4.5Cu/8μm SiC samples can also be attributed to approximately 73 times the number of SiC particulates in the matrix. This indicates the presence of a greater number of uniformly distributed heterogeneous nucleation sites when compared to the Al-4.5Cu matrix containing 34.4 μm SiC particulates even after considering similar distribution pattern. This relatively

large number of heterogeneous nucleation sites will be instrumental in facilitating easier nucleation of strengthening phases thus accelerating the aging kinetics /4,41/.

The results of the aging kinetics thus indicate that the aging kinetics of Al-4.5Cu matrix can be accelerated if the influence of SiC particulates is significant enough to bring marked microstructural changes leading to an increase in number of heterogeneous nucleation sites.

Mechanical Behavior

The results of mechanical properties characterization revealed a higher 0.2% YS and reduced UTS and ductility in case of reinforced samples when compared to the unreinforced samples (see Table 2). The higher 0.2% YS from unreinforced samples to Al-4.5Cu/34.4μm SiC samples to Al-4.5Cu/8μm SiC samples can be attributed to an increase in dislocation density in the metallic matrix. The higher dislocation density in the composite samples when compared to the unreinforced samples can be attributed to the presence of SiC particulates /2-5,38/ while amongst the composite samples the higher dislocation density in the case of Al-4.5Cu/8μm SiC samples can be attributed to the ability of finer SiC particulates to generate higher dislocation density /2/. The results of the present study are consistent with the findings of other investigators /2/ establishing that up to strain levels of 0.002, the deformation behavior that determines the tensile yield strength depends on the spacing parameters on the scale of microstructural features such as precipitates or punched out and thermally induced dislocation forests. It may further be noted that the 0.2% YS of the composite samples have been reported to increase /6/ or decrease /5, 6, 9, 43/ when compared to their monolithic counterpart primarily depending on the composition of the metallic matrix.

The lower value of UTS exhibited by composite samples when compared to the unreinforced samples can primarily be attributed to the presence of porosity in range of 4.6 to 5.78 volume percent. The porosity associated reduction in strength has been previously established by other investigators for steels, copper and aluminum based alloys /43,44/. Bocchini and Payne *et al.* /43,44/, for example, asserted that the presence of pores lead to weakening of a material by reducing the amount of stress bearing area and therefore lower the amount of stress the material is able to withstand.

Finally, the reduction in ductility exhibited by composite samples when compared to the unreinforced samples can be attributed to the reduced cavitation resistance of metallic matrix as a result of presence of porosity, SiC particulates and SiC clusters. This is in accordance with the studies conducted by other investigators /2,5,6,9,10,45/ on aluminum based metallic matrices reinforced with different types of reinforcing phases. The present study did not reveal any clear dependence of ductility on SiC particulate size.

It may be noted that the UTS and ductility values shown in Table 2 for the composite samples in the as-processed condition should be considered lower bound and can significantly be improved by eliminating porosity using thermomechanical processing techniques such as extrusion.

Fracture Behavior

The results of the fracture surface analysis indicated a relatively more brittle fracture in case of composite samples when compared to the unreinforced samples. These results are consistent with the mechanical properties results which show a significant reduction in ductility of composite samples (see Table 2). The relatively brittle fracture exhibited by composite samples can primarily be attributed to the SiC particulates associated crack initiation and the presence of porosity. The presence of SiC particulates and the associated secondary phases and intermetallics in the interfacial region /4,5,11,27/, for example, promotes early microcracking and premature failure as a result of overlapping of their plastic fields /46/. In addition, the presence of SiC particulates in the form of clusters also promote early crack nucleation as a result of high stress triaxiality generated in these regions /4,5/ and is supported by the fractographic results obtained from both the types of composite samples investigated in the present study.

Amongst the composite samples, the presence of increased number of cracked SiC particulates in the

case of fractured surface of Al-4.5Cu/34.4μm SiC samples when compared to Al-4.5Cu/8μm SiC samples can be attributed to the higher cracking tendency of the larger sized SiC particulates. In related studies /47/, for example, investigators showed using acoustic emission technique, the increased cracking tendency of SiC particulates with an increase in particulate size especially when the particulate size exceeds 12 μm.

The results of the fractographic studies conducted on the composite samples thus revealed that failure process was noticeably influenced by SiC particulates cracking in case of Al-4.5Cu/34.4μm SiC samples and particulate to matrix debonding in case of composite samples containing 8 μm SiC particulates.

CONCLUSIONS

The primary conclusions that may be derived from this work are as follows:

1. The disintegrated melt deposition route can be successfully utilized to synthesize aluminum based metal matrix composites containing SiC particulates of different sizes.
2. The increased tendency towards equiaxed grain morphology from unreinforced to Al-4.5Cu/34.4μm SiC to Al-4.5Cu/8μm SiC samples can be attributed to the increasing constraint to the growth of primary metallic phase and destabilization of solid-liquid interface by the presence of SiC particulates and the relatively superior ability of 8 μm SiC particulates when compared to the 34.4 μm SiC particulates.
3. The accelerated aging kinetics exhibited by Al-4.5Cu/8μm SiC samples when compared to the Al-4.5Cu/34.4μm SiC and unreinforced samples can primarily be attributed to the superior ability of 8 μm SiC particulates to increase heterogeneous nucleation sites in the form of increased grain boundary area, improved interfacial integrity and increased dislocation density.
4. The increase in 0.2% yield strength of the composite samples when compared to the unreinforced samples can be attributed to the ability of particulates to increase the dislocation density in the metallic matrix.
5. The results of the fracture surface studies revealed SiC breakage to influence noticeably the failure process in the case of Al-4.5Cu/34.4μm SiC samples and interfacial debonding in the case of Al-4.5Cu/8μm SiC samples.

ACKNOWLEDGMENTS

The authors would like to thank Mr. Thomas Tan, Mr. Tung Siew Kong, Mr. Boon Heng and Mr. S.B. Mong (National University of Singapore, Singapore) for their valuable assistance and for many useful discussions during the course of this investigation.

REFERENCES

1. P.S. Gilman, *J. Met.*, **43** (8), 7 (1991).
2. A.L. Geiger and J.A. Walker, *J. Met.*, **43** (8), 8 (1991).
3. I.A. Ibrahim, F.A. Mohamed and E.J. Lavernia, *J. Mat. Sci.*, **26**, 1137 (1991).
4. D.J. Lloyd, *Int. Mat. Rev.*, **39** (1), 1 (1994).
5. M. Gupta, T.S. Srivatsan, F.A. Mohamed and E.J. Lavernia, *J. Mat. Sci.*, **28**, 2245 (1993).
6. D.L. McDanels, *Metall. Trans. A*, **16**, 1105 (1985).
7. R.H. Pestes, S.V. Kamat and J.P. Hirth, *Scr. Metall. et Mater.*, **30**, 963 (1994).
8. J.J. Stephens, J.P. Lucas and F.M. Hosking, *Scr. Metall.*, **22**, 1307 (1988).
9. T.J.A. Doel, M.H. Loretto and P. Bowen, *Composites*, **24** (3), 270 (1993).
10. M. Gupta, M.O. Lai and C.Y. Soo, *Mat. Sci. Eng. A*, **210**(1-2), 114 (1996).
11. M. Gupta, C. Lane and E.J. Lavernia, *Scr. Metall. et Mater.*, **26**, 825 (1992).
12. B. Chalmers, *Principles of Solidification*, John Wiley and Sons Inc., New York, USA, 1964; pp. 253-297.
13. G.J. Davies, *Solidification and Casting*, Applied Science Publishers Ltd, London, UK, 1973; pp. 95-114.

14. M.C. Flemings, *Solidification Processing*, McGraw-Hill Book Company, New York, USA, 1974; pp. 154-157.
15. X. Liang, J.C. Earthman and E.J. Lavernia, *Acta Metall. Mater.*, 40, 3003 (1992).
16. R.H. Bricknell, *Metall. Trans. A*, 17, 583 (1986).
17. M. Gupta, F. Mohamed and E. Lavernia, *Metall. Trans. A*, 23A, 831 (1992).
18. P.S. Grant, *Prog. in Mat. Sci.*, 39, 497 (1995).
19. A. Lawley and D. Apelian, *Powder Metallurgy*, 37 (2), 123 (1994).
20. M. De Sanctis, R. Valentini, A. Solina, *Met and Mat. Trans. A*, 28 (4), 1099 (1997).
21. R.U. Vaidya and A.K. Zurek, *J. Mat. Sci. Lett.*, 15, 385 (1996).
22. J.S. Zhang, X.J. Liu, H. Cui, Z.Q. Sun and G.L. Chen, *Scripta Materialia*, 35 (9), 1115 (1996).
23. K. Murakami, A. Yoshimoto, T. Okamoto and Y. Miyamoto, *Mat. Sci. Eng. A*, 160, 137 (1993).
24. W. Zhou, Z.M. Xu, *J. Mat. Proc. Tech.*, 63, 358 (1997).
25. D.M. Stefanescu, B.K. Dhindaw, S.A. Kacar and A. Moitra, *Metall. Trans. A*, 19, 2847 (1988).
26. P.K. Rohatgi, K. Pasciak, C.S. Narendranath, S. Ray and A. Sachdev, *J. Mat. Sci.*, 29, 5357 (1994).
27. M. Gupta, L. Lu, M.O. Lai and S.E. Ang, *Materials and Design*, 16 (2), 75 (1995).
28. *Metallography and Microstructures, Metals Handbook*, 9th edition, Vol. 9, p. 632, ASM, Metals Park, Ohio, USA(1986).
29. P.K. Rohatgi, R. Asthana and S. Das, *Int. Met. Rev.*, 31 (3), 115 (1986).
30. P.K. Rohatgi and R. Asthana, *J. Met.*, 43, 35 (1991).
31. M. Gupta, F.A. Mohamed and E.J. Lavernia, *Int. J. Rapid Solidi.*, 6, 247 (1991).
32. W.D. Callister, Jr., *Materials Science and Engineering*, John Wiley & Sons, Inc., New York, USA, 1994; pp. 338-343.
33. P.G. Shewmon, *Transformation in Metals*, McGraw Hill Book Company, USA, 1969; pp. 156-309.
34. D.S. Clarke and W.R. Varney, *Physical Metallurgy for Engineers*, American Book Company, New York, USA, 1962; pp. 95-104.
35. J.M. Papzian, *Metall. Trans. A*, 19, 2945 (1988).
36. K.K. Chawla, A.H. Esmaeili, A.K. Datye and A.K. Vasudevan, *Scr. Metall. et Mater.*, 25, 1315 (1991).
37. T.S. Kim, T.H. Kim, K.H. Oh and H.I. Lee, *J. Mat. Sci.*, 27, 2599 (1992).
38. R.J. Arsenault and N. Shi, *Mat. Sci. and Eng.*, 81, 175 (1986).
39. T.S. Srivatsan, M. Gupta, F.A. Mohamed and E.J. Lavernia, *Aluminium*, 68, 494 (1992).
40. M. Taya, K.E. Lulay and D.J. Lloyd, *Acta Metall. et Mater.*, 39, 73 (1991).
41. M. Gupta and M.K. Surappa, *Mat. Res. Bull.*, 30 (8), 1023 (1995).
42. M. Gupta, L. Lu and S.E. Ang, *J. Mat. Sci.*, in press, 1997.
43. G.F. Bocchini, The Int. J. of Powder Metallurgy, 22 (3), 185 (1986).
44. R.D. Payne, A.L. Moran and R.C. Cammarata, *Scr. Metall. et Mater.*, 29, 907 (1993).
45. M. Gupta and M.K. Surappa, Key Engineering Materials, 104-107 (Part 1), 259 (1995).
46. D. Kwon and S. Lee, Key Eng. Mat., 104-107 (Part 2), 655 (1995).
47. Z. G. Wang, S. Li and L. Sun, Key Eng. Mat., 104-107 (Part 2), 729 (1995).